

Thermally Actuated Mobile Structures

The design of silicon based, integrated mechanical structures has resulted in the technology called MicroElectroMechanical Systems or MEMS. We propose to create a new class of structures that would be free to move over a surface, and eventually, be capable of moving in 3 dimensions. The uses of these freely moving structures would be to manipulate, place or remove objects on a surface. With a nano-tool fabricated on the mobile structure, they could be used to assemble components of smaller systems, repair failed circuitry, clear debris or retrieve nano-particles or molecules for analysis. In the simplest case, they may consist of very simple shapes such as triangles, and their actuated motion would be caused by a uniform temperature change. In the case with the greatest control, the structure would be designed with independently actuated arms, able to translate, rotate and manipulate other objects. The individual arms would be independently addressable, and the position and shape of the structure would be detected and controlled in a closed loop system. There are many ways in which the field of MEMS has actuated structures, including electrostatic, magnetic and thermal. In this proposal we propose to focus on thermal actuation because it offers a way, through optical excitation, to actuate independent parts of the structure with the versatility of controlling wavelength and temporal profiles. We therefore call these structures TAMS, for thermally actuated mobile structures.

Our research program, extending over 3 years, is designed to design, model and demonstrate mobile systems. How does the scaling down to nanoscale structures affect the tradeoffs between thermal management, stiction, optical excitation, force generation and mechanical response time? What are the design considerations for mobility in complex versus simple shapes? We divide our program into three components:

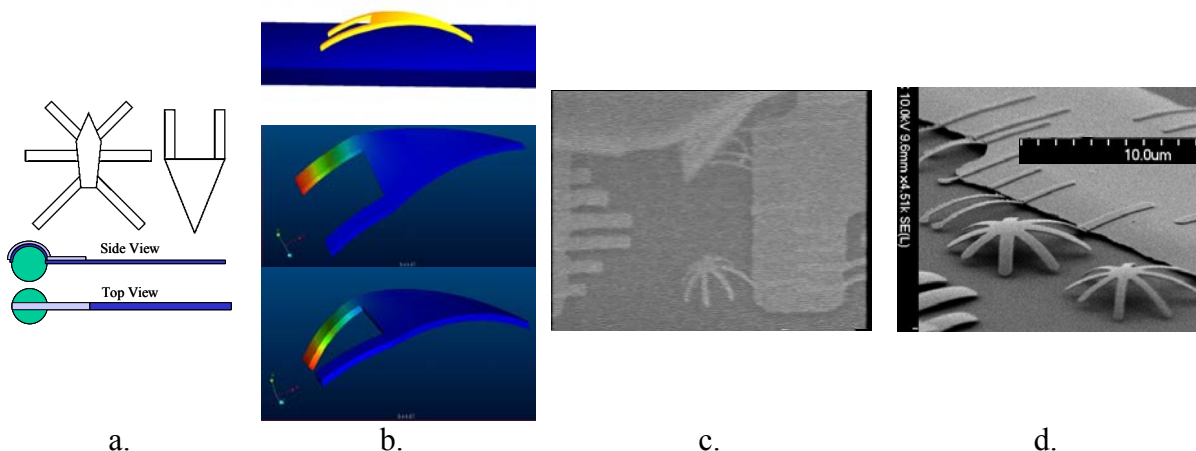


Figure 1. Schematic of TAMS. a) top view of simple two-legged “seal” and six-legged “ant” for 2D motion, and a bead with bimetallic flagellum for 3D. b) projected view of prestressed seal-TAMS with body up off surface. Drawings of heat induced change in one leg of seal optically heated to curl under TAMS by slip. Subsequent relaxation of leg would propel or rotate structure (*colored pictures, not a simulation*). C. SEM of AFM tip poised over field of TAMS in our combination SEM/AFM, with d) enlargement of a 8-legged TAMS designed to be precurved.

1. Design and Development (Superfine, entire team): This includes the design, fabrication and characterization of a first generation of TAMS for 2d and 3d motion starting from two classes of shapes: a. simple shapes such as triangles and b. complex shapes such as legged structures. We will employ photo- and electron beam lithography with thin film deposition of common materials such as Si, SiN, Polyimide as well as metals such as Cr, Al and Au. Our characterization will include thermal (i.e. optical) excitation within an SEM, including time resolving the dynamics. Our goal will be to demonstrate actuation and mobility of these structures, to understand the design principles for actuation and dynamics.

2. Nanoscale thermal actuation materials and Processing (Stoner, Falvo): One of the most recent developments in thermal actuation is the application of shape memory alloys. These materials use a phase transformation to provide strains much larger than can be provided by a single material with linear thermomechanical properties. Clearly, the scaling laws of thermal actuation can be dramatically different if SMAs can be employed. We will study the submicron film limits of the thermomechanical behavior of SMA materials such as TiNi alloys, and inject these films into our processing of TAMS. A second class of materials of interest for thermoactuation are nanotubes and nanorods. These materials, available in diameters down to less than 1nm

composed of carbon, silicon, Si_3N_4 and other semiconductors, offer a route to scaling actuating structures to the molecular scale. We will study the actuation of individual nanotubes including the control over bi-material asymmetric coatings. We have succeeded in producing curved bi-film structures with carbon nanotubes using colled coatings. Difficult scaling issues include the diffusion of deposited material around the circumference of the nanotube and the effect of grain size on thermomechanical properties.

3. Modeling (Seelecke): The computation of the thermomechanical effects, including the structural deformations and the temporal evolution of the thermal distribution will be essential for the understanding and design of these systems. We will perform finite element calculations of the dynamic behavior of bimaterial structures (including SMA materials) incorporating, from the outset, the thermal coupling to the ambient. Subsequent models will include the effects of thermal coupling to the substrate through small contact points. Later, the incorporation of van der Waals forces will be critical for the consideration of the scaling of TAMS to the nanoscale. By the end of the grant period we expect to incorporate stiction effects so that we may have full simulation capability of thermally actuated mobile structures.

Distinguishing Capabilities

We will make use of several enabling experimental capabilities that have been developed at UNC. Our team includes Dr. Brian Stoner and his group at the MCNC for growth, advanced processing and device analysis.

Combination SEM/AFM manipulation system: For the characterization of surface forces that affect mobility, such as adhesion and stiction, we will employ our advanced interface for scanning probe microscopy that applies advanced data rendering, image analysis and real-time control into a powerful system for nanoscale science [Taylor1999]. The user can perform intuitive AFM manipulations by controlling the position of the AFM tip using a pen-based control. The scientist holds a stylus and, by moving their hand, translates the AFM tip over the sample with a magnification of over 1 million. We use this manipulation capability within our combination SEM/AFM system. (Fig. XXX) We can manipulate and perform force measurements for stiction (See Fig. XXX) and mechanical properties with an AFM with simultaneous viewing in our Hitachi S4700 field emission, 2nm resolution SEM. Preliminary results of these studies are discussed below.

Combination TEM/manipulation system: We have been awarded a grant from the W. M. Keck Foundation for the development of a user-guided atomic resolution manipulation system. We are installing a high resolution TEM (JEOL 2010F-200kv field emission) that will allow atomic resolution studies of SMA thin films and nanotube/thin film interfaces. We are designing MEMS stages for manipulation and characterization capability correlated with TEM imaging, including thermal actuation and force measurement.

3D Force Microscope: We have designed and developed under NIH funding a new 3D force microscope that applies forces to a paramagnetic bead using designed magnetic fields, while tracking the bead to nanometer, millisecond resolution using laser light scattering. We will use this system to trap and track magnetic beads that will be fabricated with micropatterned flagella. (See Fig. XXX)

Leveraging Resources

This project coordinates with several allied research efforts that add great strength to our group.

The nanoManipulator Project: This multidisciplinary effort of Computer Scientists, Physicists, Chemists (among others) pursues advanced interfaces in microscopy. It is funded through several grants including an NIH NCRB for biosciences applications as well as DOD funding. The nM project will indirectly provide microscopy interfaces, control and data analysis for the AFM/SEM (See Fig. XXX), while the NIH center supports the development of the 3DFM that will be used for studying 3D actuating structures.

MCNC: A major partner in this research is the processing, design and characterization expertise available at MCNC (formerly the Microelectronic Center of North Carolina). MCNC, established by the North Carolina Department of Commerce in 1980, has developed a core expertise in the design, microfabrication, and analysis of microelectronic devices and integrated systems. The Materials and Electronic Technologies Division (METD) of MCNC, with a staff of about 27, has programs in the technology areas of Sensors and Actuators, Wireless Communications, Advanced Packaging and Interconnect, Electronic Materials and Microstructures, and Analysis and Fabrication. In the 1990's MCNC established a core expertise in the design and fabrication of MEMS.

1. Design and Development

Actuation

Introduction: The actuation of MEMS devices has been accomplished using electrostatic, magnetic and thermomechanical forces. We envision TAMS as untethered structures, free to move about a surface. This necessitates a coupling to the device that does not impose mechanical constraints. Electrostatic and magnetic forces can be applied to an untethered microstructure only through the application of a potential to the substrate or to the immersion of the sample in a magnetic field. This would make the selective coupling to specific legs within a device quite difficult. Optical coupling offers many opportunities for tailoring the temporal profile through pulse shaping, the spatial profile through focusing or image projection, and absorption through wavelength and polarization. For these reasons, we have chosen opto-thermal actuation of TAMS.

Shape: General Considerations – The choice of shape has implications for the complexity of the control system and for the sophistication of device performance. We envision two classes of shapes, and two classes of thermal profiles.

• **Shape 1: Simple Figures** –

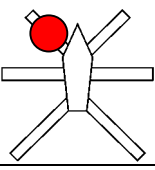
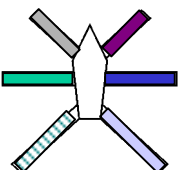
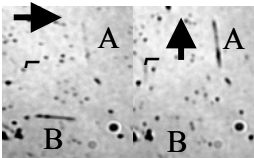
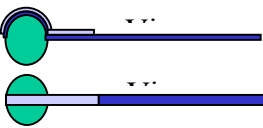
While it is natural to begin the consideration of legged structures, it is interesting to ask: What is the simplest figure that would exhibit thermally actuated motion? For example, would an elongated triangle that is uniformly heated, perhaps with an impulse energy deposition that produces a temporal profile with a sharp rise and relatively slow decay, translate along the surface? Can a symmetric figure be induced to move through a spatially asymmetric thermal profile? Such simple shapes may be available for manufacturing from relatively simple processes derived from colloid chemistry, self-assembly or stamping procedures. Such shapes placed onto a surface may have limited functionality, but may play an intriguing role in, for example, wafer cleaning or as fundamental elements for surface self-assembly. We will explore the actuation of simple shapes to understand the limit in terms of geometrical complexity.

• **Shape II: Legged structures** –

Legged structures offer biomimetic strategies for locomotion and the possibility that legs may act as tools in addition to propelling the structure. There have been detailed studies of insect locomotion and how they sequence their legs, turn and run [Full1997] [Dickinson2000]. Similar strategies, with appropriate actuation of the legs, may provide insight into mobility design.

Thermal profiles: General Considerations – As in the decision of appropriate shapes, the question arises as to what form of thermal profile is necessary for locomotion.

- **Thermal Profile I: Uniform** - In the simplest case, it is possible that a uniform temperature rise of the TAMS will provide locomotion. Locomotion presupposes some form of asymmetry, spatial or temporal, so that the structure does not return to its same position after cycling back to room temperature. The asymmetry in the case of uniform illumination would be temporal: a sharp rise in temperature due to the absorption of a short laser

Heating	Illumination	Absorption	Mech. Struct.	Shape Control Strategies: Examples	
P	P	U	U		A simple spider shape from lithographically patterned Cr/Au. Laser is focused onto one leg to achieve bending.
P	U	P	U		Spider with wavelength selective absorptive films patterned onto each leg. Illumination is broad, with only tuned leg heating.
P	U	P	U		Antenna effect I: Only nanotube parallel to light polarization absorbs and bends. Use polarization to select orientation of bending leg.
U	U	U	P		A bead with microfabricated flagella patterned to have only first section “bimetallic”. Wave initiates in this region and propagates.
Figure. XXX. Shape control mechanisms. P: patterned, U: uniform. Except for first example, the actuation uses broad (unfocused) illumination.					

pulse, followed by the slower temperature drop as the heat is carried off into the ambient or into the substrate. The fast temperature rise produces a mechanical response on the time scale of the resonance frequency that may allow contact points to slip. The subsequent slow relaxation would produce an overall dynamics that would be determined by the competition between the stiction constraining contacting points. Alternatively, we may tailor actuation in a given leg through a proscribed SMA transition temperature, different for each leg. This will be described in the section on advanced materials.

- **Thermal Profile II: Structured** – The most complex control over actuation will come from structuring the light so that different parts of the TAMS can be independently actuated. In the section on the optical control of TAMS, we will discuss strategies for the control of focused light on the sample.

How are they going to move?:

1. Stick Slip: The process begins with the change in the shape of the structure through a change in temperature. In the structures we envision they are processed with built-in stress that produces a curvature upon release that allows the TAMS to have its body off of the substrate, supported by its legs. Upon a fast heat step, the leg will curve further under the TAMS, tilting it on the surface. There are two possibilities that can occur: a) the actuated leg(s) slip with the other legs remaining in place, or b) the actuated leg(s) remain in place while the other contact points slip. Similar considerations will apply for other shapes and leg configurations. In a simple analysis where we consider the friction force as having a threshold force for slipping, the motion that required the least force would be realized. For example, in the case of the seal-TAMS with three contact points, the actuation of one leg would result in that leg slipping, since this would require less force than simultaneously sliding the other two contact points. In the case where the two legs are actuated simultaneously, the triangular point would slide. These motions are also consistent with energy considerations, where the energy lost to friction is simply $U_f = A_c \sigma_f$, where A_c is the area of the contact, and σ_f is the surface stress describing the friction [Falvo2000a]. The actuated leg, heated with a microsecond scale laser pulse, would perform a slip motion due to the friction forces that constrain the other legs and the inertia. This competition between the inertia of the TAMS and the slip of the actuated contact point can be described by the inequality $F_{move} > F_f$. If F_{move} , the force required to accelerate the entire structure within the time frame of the thermally induced bending, is greater than the force due to friction at the contact point F_f , then the actuated contact point will slip.

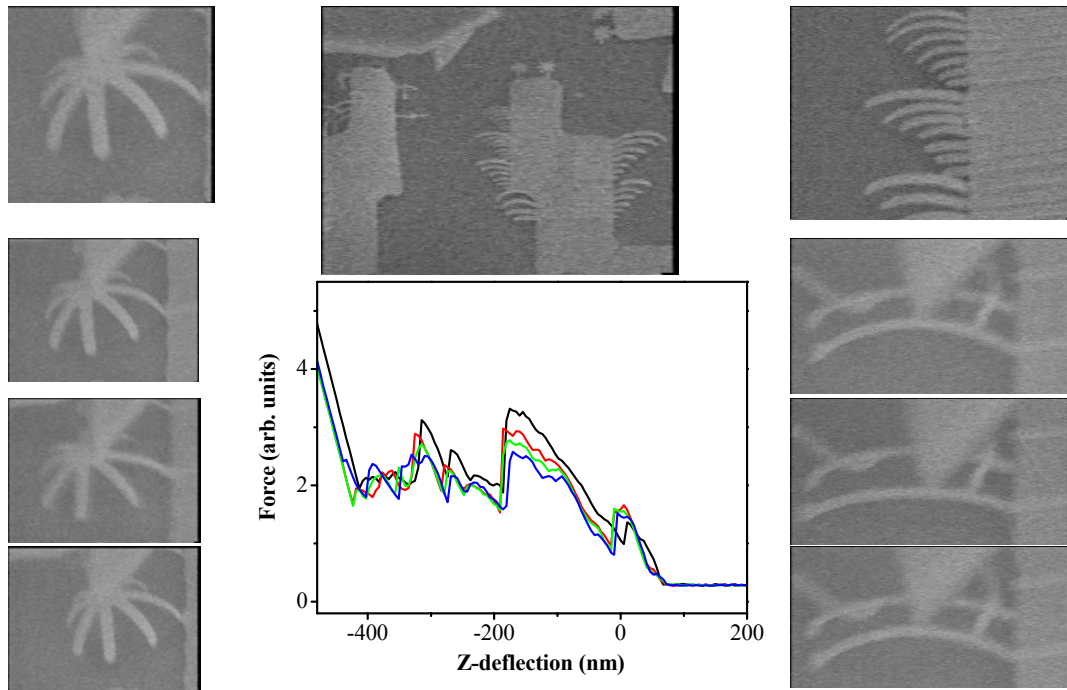


Figure XXX. Left: Sequence of pressing on spider structure with AFM tip showing the slip of the spider legs across the surface and the ability of the structure to resume its shape against stiction forces when the pressure is released. Top: AFM tip hovering over e-beam lithography stiction test structures. Top Right: Zoom on row of test strips. Right: sequence of AFM force stiction cycles as the tip presses on a beam, and release. Middle above: AFM force curves measured during stiction test cycles showing sawtooth features characteristic of stick-slip phenomena.

We can generate a simple expression for $F_{move} = m a_{max}$ if we assume that the TAMS responds on a time scale Δt consistent with its resonant frequency f , and moves through a distance Δx , the deflection of the actuated leg. We assume a simple velocity profile $v = v_o \sin(2\pi ft) = (\pi\Delta x/2\Delta t)\sin(\pi t/\Delta t)$, and the object finishes the motion at time $t = \Delta t$. The differentiation of this expression yields the maximum acceleration, $a_{max} = (\pi^2/2)(\Delta x/\Delta t^2)$. We can estimate the timescale of the response of the TAMS by the calculating the resonance frequency characteristic of a beam of the approximate dimensions of the TAMS. We take a cantilever beam with a length L , thickness h , Young's modulus E and density ρ , and obtain $f = \frac{1.02}{2\pi} \frac{h}{L^2} \sqrt{\frac{E}{\rho}}$. For a TAMS with $L = 10\mu\text{m}$, $h = .1\mu\text{m}$ made of gold with $E = 78 \text{ GPa}$ and $\rho = 19,300 \text{ kg/m}^3$, we obtain $f = 325\text{kHz}$, corresponding to a $\Delta t = 1.5\mu\text{sec}$. The force needed to accelerate the TAMS on this same timescale is given by $F_{move} = m a_{max} = \rho Ltw(\pi^2/2)(\Delta x/\Delta t^2)$. If we take our TAMS to have a width $w = 4\mu\text{m}$, with the thermal excitation producing a $\Delta x = 50\text{nm}$, and $\Delta t = 1.5 \mu\text{sec}$ as calculated above, we find that $F_{move} = 8\text{nN}$. This value should be compared with the force due to friction at a nanoscale contact, where $s = 1\text{Mpa}$ (typical for a low friction interface) and a contact area of $30\text{nm} \times 30\text{nm}$, we find a $F_f = 1\text{nN}$. Under these conditions, $F_{move} > F_f$ and the contact point with the fast thermal heating will slip while the remaining structure can be expected to stay fixed.

The above arguments are rife with assumptions about contact areas, interfacial shear stresses, the TAMS mechanical response time and the dynamics of sliding. However, they put into context the competition between these phenomena and how the physics of mobile structures may scale into the nanoworld. These considerations will

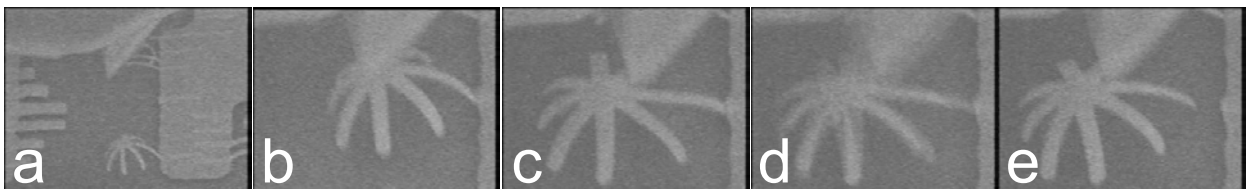


Figure 2. Release and manipulation of TAMS: This sequence shows (a) the AFM tip over the spider TAMS in our SEM/AFM system. The tip then (b) contacts the spider, and stresses the thin connecting bridge (c), finally releasing the spider (d) from its support leg. The spider is then slid away (e). This procedure demonstrates our ability to create complex shapes and post-processing, and to perform lateral force measurements of the friction/stiction of these structures against a surface.

also guide our choice of TAMS geometry (small contact points), surface treatment, resonance frequency and the role of the optical temporal profile in actuation. With our experimental capabilities, we will be able to measure the force of stiction and friction on our TAMS directly. We have the capability within our SEM/AFM system to perform quantitative measurements on the forces required to move TAMS laterally. We have done so in experiments that have elucidated the atomic scale effects in the dynamics of carbon nanotubes on surfaces [Falvo1999, 2000a, 200b]. Within this project, we will manipulate TAMS with our SEM/AFM system to measure the stiction directly. A preliminary manipulation shown in Fig. XXX, shows the probing, separation and translation of a spider structure (Au on Cr) released on silicon. The structure is prestressed by interfacial stresses inducing a curvature that lifts the center off the substrate.

2. Circular trajectory: Insects move by actuating legs independently by releasing legs in sequence from the substrate, moving them forward, reattaching to the substrate then pushing the leg backward [Full1997][Dickinson2000]. During this cycle, there is no stick slip phenomenon. Can we replicate this motion by controlling the thermal cooling timing so that leg has sequenced normal and lateral motions? Thermal actuators have been designed for either in-plane or out of plane motion using both bimaterial structures and structures with two different thermal transport properties. We will attempt to design structures that combine both features to create a circular motion. For example, a bi-leg structure from a bimaterial layer may use the out-of-plane bending of the entire structure from the differential coefficients of expansion, while the in-plane bending would occur from the difference in temperature between the thick and thin legs. If we can induce a leg to follow a circular trajectory, then we will proceed with the appropriate sequencing of the legs through the timing of optical spots on the TAMS.

Thermal Excitation of Actuation

Understanding the thermal bending of the TAMS will be essential to produce the movement of the structure over the surface. We will study the thermal response of our structures in three ways:

1. We will pattern TAMS with patterned metal film wires that connect the TAMS to leads that will be connected to external circuitry. By applying a current to the metal connection, we will heat the wire and the connected TAMS. The calibration of the temperature will be done by calibrating the resistance of the wire in a separate experiment in a thermostated environment, with the resistance measured in a 4-probe geometry (see Fig. 4). The test structure will then be placed in the SEM and a current applied. We will then measure the bending of the structure through SEM imaging as a function of the wire resistance, and therefore, temperature. We can then heat these test structures through optical excitation (see below) and compare directly with the resistively heated bending.

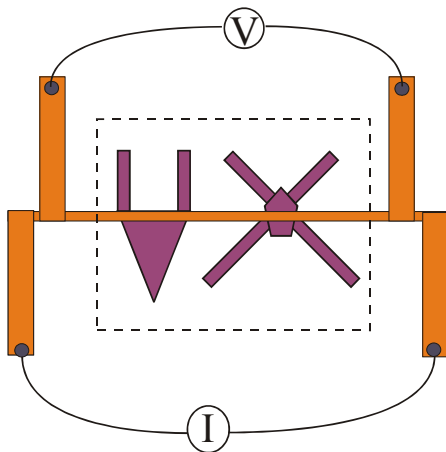


Figure 4. Joule heating test structure with all colored boxes joined, purple denotes the TAMS. Region inside dotted box is released so that thermal tests and bending tests can be performed inside SEM

2. In the next test, we will place the separated TAMS on the substrate inside the SEM and observe the bending and actuation under optical (laser) illumination. Our combination SEM/AFM provides a versatile platform for designing a variety of sample holder stages with external electrical and optical inputs. Through a remote window, it is quite simple to provide illumination with controlled polarization. The spot size through a remote window would be no smaller than about 15 microns, and so focusing on specific legs would be impossible. To do this, we would need to place an optic close to the sample. We have a convenient system in place in the form of our AFM that provides us with a 650 nm laser inside the SEM, and the ability to move the sample under the laser spot with nm resolution. This capability will allow us to test optical actuation within the SEM.

3. Finally, we will move the TAMS to ambient conditions. We will excite the bending of test structures under an optical microscope and use the resistively heated structures from test 1 above and the separated TAMS from test 2. For quantifying the beam deflection, we will consider establishing an interference microscopy system, or gain access to test facilities at MCNC.

Dissipation of heat from the TAMS is a particularly intriguing question. TAMS are in contact with the substrate only through small areas at a few points, so much of the dissipation is in the form of internal mixing of modes and radiation to the environment. Depending on the choice of constituent materials, we may find thermal transport mechanisms in the diffusive regime where Fourier's heat applies or in the ballistic regime. Diffusive thermal transport is expected in all granular metal films and so in the SMA films, but carbon nanotubes are expected

to respond more or less as ballistic systems under modest heat loads and 500nm thermal mean free paths have been observed [Kim2001]. Radiative dissipation from the structure

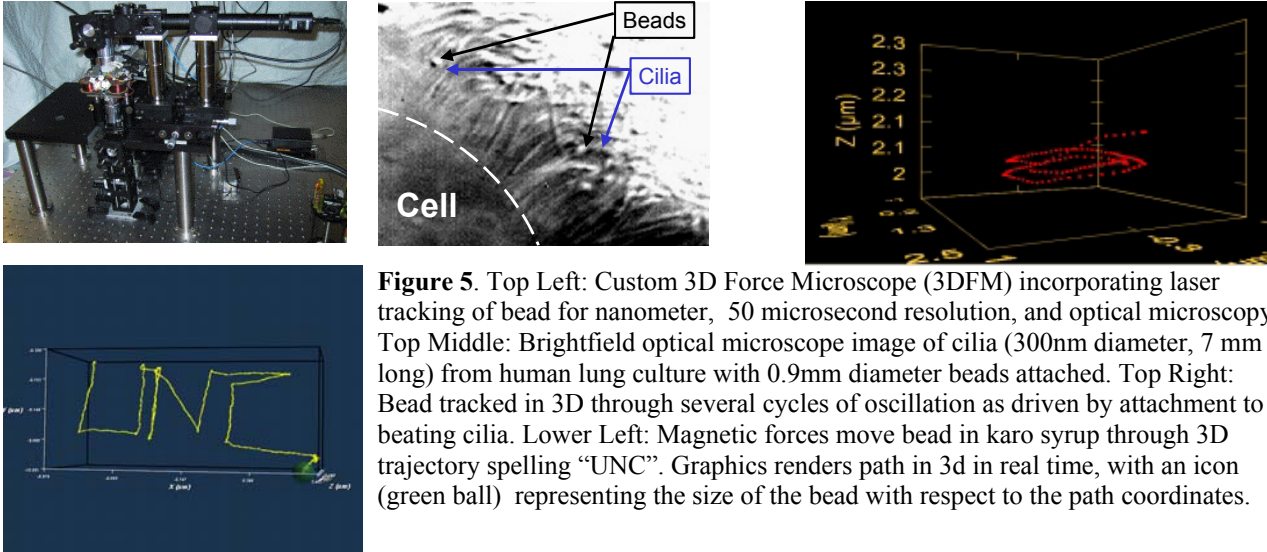


Figure 5. Top Left: Custom 3D Force Microscope (3DFM) incorporating laser tracking of bead for nanometer, 50 microsecond resolution, and optical microscopy. Top Middle: Brightfield optical microscope image of cilia (300nm diameter, 7 mm long) from human lung culture with 0.9mm diameter beads attached. Top Right: Bead tracked in 3D through several cycles of oscillation as driven by attachment to beating cilia. Lower Left: Magnetic forces move bead in karo syrup through 3D trajectory spelling “UNC”. Graphics renders path in 3d in real time, with an icon (green ball) representing the size of the bead with respect to the path coordinates.

into the environment is simple to describe in principle but very difficult to estimate quantitatively. It is the integral over the surface area of the structure of a product of a (possibly temperature-dependent) radiation probability (or emissivity) and the deviation of the fourth powers of the local temperature of the structure from the environment temperature. This loss may provide the bottle-neck to dissipate the applied heat for *in vacuo* studies, and the application of the joule heating test rig in the SEM may help separate radiative losses from conduction to the surrounding fluid. For almost all structures we expect heat to be dissipate through thermal contact to the surrounding fluid or to the substrate through points of support.

For diffusive thermal transport, we may assert that the thermal relaxation occurs on time-scales of order L^2/D where L is the length of the region and D is the thermal diffusion coefficient (diffusivity) of the material. $D = \kappa/c\rho$ where κ is the thermal conductivity, c is specific heat and ρ is the density of the material. For common metals, $D \approx 1 \times 10^{-4} \text{ m}^2/\text{s}$, and for silicon, $D \approx 1 \times 10^{-5} \text{ m}^2/\text{s}$, and for an insulator like SiO_2 , $D \approx 1 \times 10^{-7} \text{ m}^2/\text{s}$, but on the other hand for carbon nanotubes the relevant scale is not a diffusion parameter but the thermal phonon speed but reduced to a comparable form (such as for a large diamond), $D \approx 1 \text{ m}^2/\text{s}$. Immediately this spread of values means that thermal gradients will exist across the structures for modest time-scales. For insulators, the time scale can be as long as 10 μs , but that time will drop dramatically for carbon nanotubes. The quantity of interest is the ratio of the thermal relaxation time to the mechanical response time. This ratio can be adjusted by changing the shape and size of the devices, since D does not depend on sample dimension, where as the mechanical response is proportional to L^2/h . For example, we calculated above that the mechanical response time for a 10 μm length TAMS to be 1.5 μsec , whereas the thermal relaxation time from the above considerations for a silicon TAMS would be about 10 μsec . The thermal excitation would be localized long enough for the leg to respond and change its shape. We expect therefore to be able to actuate the devices by applying heat (focused light) on isolated regions of an individual TAMS or by blanket illumination. The shape and size of the particular TAMS will decide the choice between these two methods.

As in the case of the motion of a TAMS, the thermal considerations contain many assumptions, yet provide guidance for the design and scaling of the test structures. Our measurements will be compared to, and modify, the detailed modeling that will be performed with in the proposed research as discussed in a later section.

Optical Excitation

We propose to use light to create thermal profiles in the TAMS to control its shape. There are a variety of ways in which light can be controlled to create diverse profiles. First, the light from a laser can be focused to a spot, with the position of the spot determined by a tilt mirror in the back focal plane of the objective. The position of this spot can be changed with bandwidths greater than 1kHz [GSI2001] [Mio2000]. Faster bandwidths would be available with acousto-optical deflection. The ultimate optical control system, with the potential ability to control multiple TAMS simultaneously would be to create an image of the desired sample optical field in the conjugate plane of the objective. A digital light processing array or a liquid crystal shutter, for example, could program this image. In the context of this proposal, we will implement a simple scanned laser spot system for the quantitative testing of TAMS. This testing will take place in our SEM as well as an optical microscope. High speed, high resolution testing of opto-thermal TAMS actuation will be studied using time-resolved SEM imaging. This can be accomplished by synchronizing the video signal with the excitation pulse, and has been applied to studying the resonant modes of MEMS beams at frequencies exceeding 300kHz [Ogo1996].

A second class of optical excitation is to use a broad uniform beam and to control the absorption in the TAMS through polarization and wavelength. No tracking of the TAMS would be necessary. The leg of the TAMS

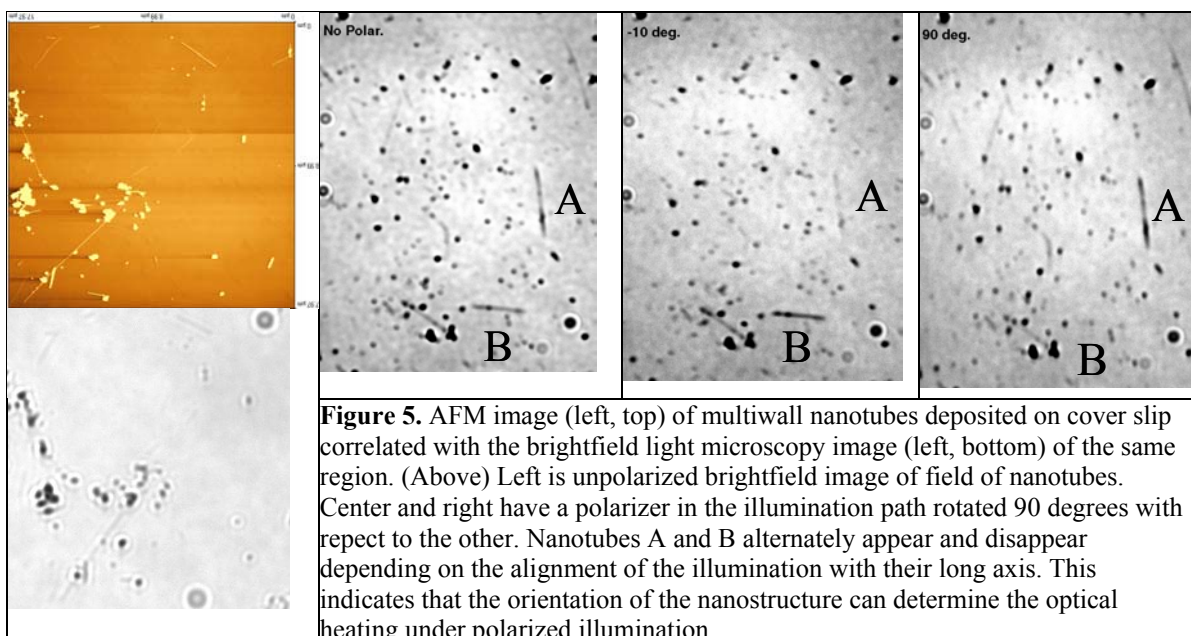


Figure 5. AFM image (left, top) of multiwall nanotubes deposited on cover slip correlated with the brightfield light microscopy image (left, bottom) of the same region. (Above) Left is unpolarized brightfield image of field of nanotubes. Center and right have a polarizer in the illumination path rotated 90 degrees with respect to the other. Nanotubes A and B alternately appear and disappear depending on the alignment of the illumination with their long axis. This indicates that the orientation of the nanostructure can determine the optical heating under polarized illumination.

would be selected through the color and polarization of the broad illumination. As the TAMS is scaled from the micron to the nanoscale size, selective focusing becomes increasingly difficult, and a broad beam strategy will be more attractive. If we consider the four legged TAMS, two legs could be 500 nm long, while two could be 625 nm in length. Each pair of similar length legs would be arranged 90° with respect to each other, as in Fig. 4. For legs that have a significant aspect ratio, the absorption in the leg parallel to the optical polarization should be significantly larger than that of a leg oriented perpendicular. Further, we should be able to design wavelength selectivity of the legs through absorptive coatings or through the antenna effect [Einarsson 1987]. For the latter, the scattering of parallel light is greatest when the length l of the leg is an integer multiple of one half the wavelength of the light. For example, average backscattering cross section for thin wire scatterers can be larger by a factor of four for $l=\lambda/2$ versus $l=1.5\lambda/2$. We will study the polarization and antenna phenomena in TAMS and in nanotube/nanorods materials. Figure 5 shows data collected from Atomic Force Microscopy and from optical microscopy. Nanotubes, averaging 20nm in diameter, lengths ranging from under 500nm up to over 5 microns are deposited on the surface and we obtain correlated optical AFM images for detailed analysis of the light scattering. Also shown in this figure is the polarization dependence of the light scattering, indicating that legs may be selected for heating by properly aligning the light polarization. Previous studies have shown enhanced Raman and Rayleigh scattering when the incident optical field is polarized along single wall nanotube bundles [Yu2001][Jorio2000]. No

study has yet showed the resonant antenna effect in nanotubes. We will perform studies of the optical scattering in TAMS using wavelength selective, polarized microscopy, as well as polarized excitation within the SEM. This will enable us to image the actuation correlated with the light scattering.

2. Nanoscale thermal actuation materials and Processing

Advanced Materials, Patterning and Processing: Photo and Ebeam Lithography

We will employ, at the outset of the project, conventional thin films in bilayer structures, for thermal bending. The equation (1) for the bending of a thin, bilayer beam guides the choice of materials:

$$d = 3(\alpha_1 - \alpha_2) \left\{ \frac{t_1 + t_2}{t_2^2} \left[4 + 6 \left(\frac{t_1}{t_2} \right) + 4 \left(\frac{t_1}{t_2} \right)^2 + \frac{E_1}{E_2} \left(\frac{t_1}{t_2} \right)^3 + \frac{E_2}{E_1} \left(\frac{t_2}{t_1} \right) \right] \right\}^{-1} \Delta T l^2 \quad (1)$$

where d is the deflection of the lever's tip, t_i is the thickness of the layer ($t_{Cr} = 20\text{nm}$, $t_{Au} = 100\text{nm}$), α_i is the expansion coefficient, E_i is the Young's modulus ($E_{Cr} = 2.79 \times 10^{11} \text{ Nm}^{-2}$, $E_{Au} = 0.8 \times 10^{11} \text{ Nm}^{-2}$), ΔT is the

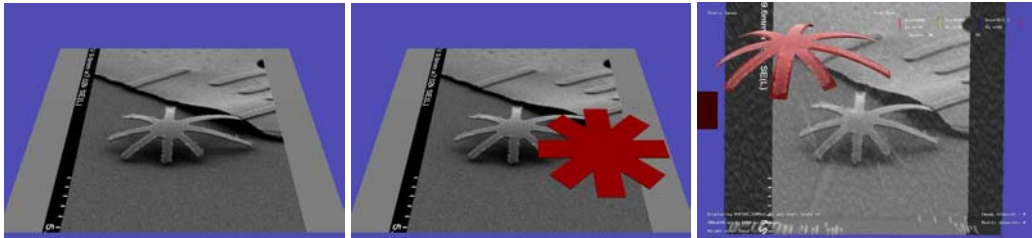
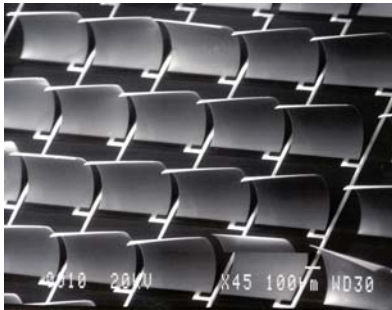


Figure XXX. Shape analysis tools. We have developed a graphics tool for quantitatively assessing the curved shape of an object from an SEM image. Left: Original SEM image of curved spider. Middle: Rendering of superimposed geometrical shape. The user has control to alter length and width of each leg, and subsequently to assign curvature to each leg. Ideally, the assignment of the dimensions of the structure will be assigned from a top-down image before pattern release. Right: Finally, the perspective of the SEM image is then used determine the leg curvatures and to project this geometrical form onto the SEM image. Note the overlay of the SEM image with a transparent rendering of the geometrical form.

temperature change along the length of the lever, and l is the length of the lever. For the maximum deflection for a given temperature, it is clear that one wants materials with the greatest difference in coefficient of thermal expansion. Materials such as Si ($\alpha_{Si} = 2.6 \times 10^{-6} \text{ K}^{-1}$), SiN and chromium ($\alpha_{Cr} = 4.9 \times 10^{-6} \text{ K}^{-1}$) offer low α_i , while gold ($\alpha_{Au} = 14.2 \times 10^{-6} \text{ K}^{-1}$) and polyimide ($\alpha_{PI} = 57 \times 10^{-6} \text{ K}^{-1}$) offer high α_i . Polyimide has been used with an SMA alloy (TiNi, $\alpha_{TiNi} = 6 \times 10^{-6} \text{ K}^{-1}$) for thermal actuation [Gill2001], taking advantage of the large mismatch in these materials.



The initial shape of the TAMS will be essential for freeing the structure from the surface. Much effort has been expended in the MEMS community for the control of residual stress that contributes to the initial distortion of structures. Largely this effort is directed at *reducing* residual stress to leave structures flat. Our goal will be to control this stress in order to create curved structures that will leave the body of the TAMS off the surface, with the legs touching. We will draw on the experience of MCNC in stress-controlled shape processing. At left, an example of a microfabricated “eyelid” that relies on the compressive stresses in a polymer layer to cause curvature and opening of the shutter. This stress-driven curl process is similar to that which is expected for the mobile, TAMS actuators, from traditional materials or from SMA-based actuators

[Gill2001]. Our processing and materials choices will take into account the process-related stresses (largely temperature effects) and material-dependent interfacial stresses to produce precurved structures. Our preliminary data shows that we have been successful in creating “spider” structures from simple Au on Cr layers, with critical point drying releasing (see Fig. 1).

Advanced Materials

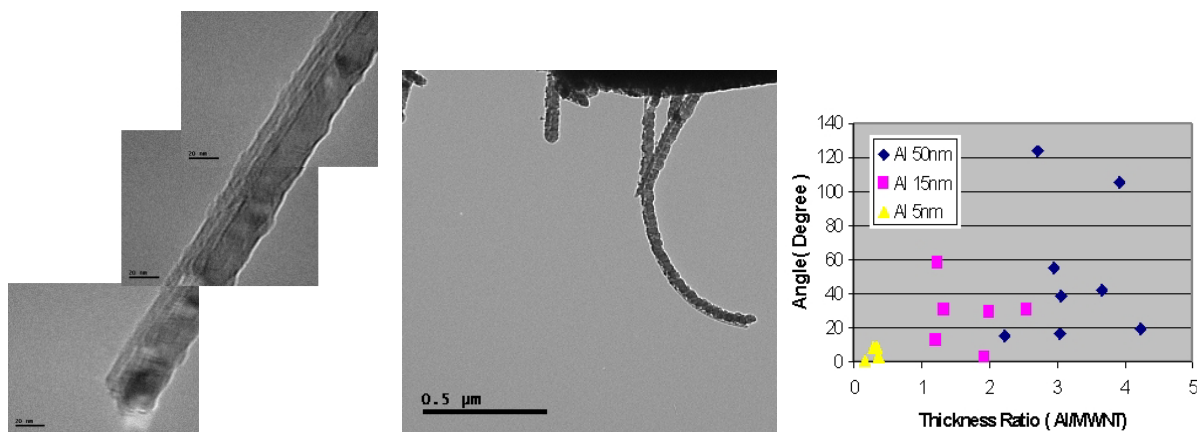


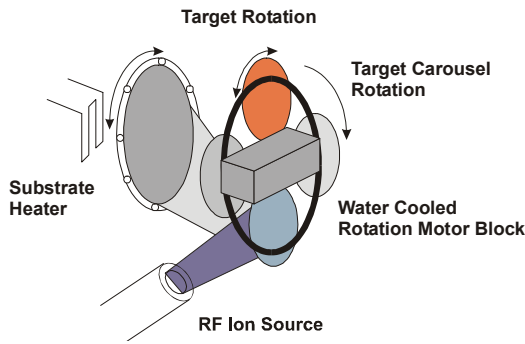
Figure 6. Preliminary data. Left: TEM Carbon nanotube with aluminum cold-deposited single-sided layer. Nanotube, with central open tube, can be seen to left, metal film to the right. Middle: Carbon nanotube/metal structure bent by interfacial stresses. Right: Plot of CNT/Metal curvature as a function of the ratio of the CNT diameter to the metal film thickness. It is expected, if the film properties scale to nanometer thicknesses, that the points should follow equation (1) with a rise to a peak at a thickness ratio determined by the relative mechanical properties of the two materials.

Nanorods and Nanotubes: We will use a variety of nanotubes to test the deposition and thermal actuation. These include carbon multiwall and single wall nanotubes, Si (with SiO₂ outer layer) nanorods and Si₃N₄ nanorods. The mechanical properties of such rods are a challenge to measure [Lieber1997]. We have developed sophisticated techniques for manipulating individual nanotubes with quantitative force microscopy for performing such measurements [Falvo1997].

The design of nanoscale thermal actuators based on bimetallic structures presents the challenge of controlling the placement of material against the influences of diffusion during the deposition process and migration during structure actuation. We have begun the study of thin metallic films on nanotubes. In Figure 6 we demonstrate the coating of carbon nanotubes with gold, chromium and aluminum. It is observed that gold films tend to migrate around the entire circumference of the 20nm nanotube, whereas thin chromium and aluminum layers tend to remain on the side of the incident material flux. We have also observed the effect on grain size for the optimal coating. Our most successful single-sided coatings have come from Al deposition on a liquid nitrogen cooled sample stage. We have analyzed a set of films to understand the curvature induced by the processing, presumably from interfacial stresses. The thermomechanical properties of these thin films on the nanotubes will be studied with an in-situ heating stage inside a. our SEM/AFM and b.our atomic resolution TEM. These studies will be correlated with mechanical measurements performed with our AFM that will separately measure the bending stiffness of these structures. We believe that these will be the first tests of the thermomechanical properties of nanotube composite structures.

Shape Memory Alloy Thin Films: Thin-film TiNi alloys developed for MEMS applications were reported by Walker and co-workers in the early 1990's [Walker1990]. Subsequently many groups have been interested in the large actuation work densities that can be achieved through the fabrication of microfluidic and other MEMS structures [Kahn1998]. Earlier this year, Shih and co-workers reported on the processing issues associated with creating a reproducible, robust MEMS structure [Shih2001]. They demonstrated that small variations in stoichiometry can significantly alter the transformation temperature of the SMA structures. (eg. Shifts of several percentage points can adjust the transformation temperature from 40 to 100 C). These and related reports highlight the need to carefully control the deposition and post-processing environment. Impurities and processing ambient can significantly affect the performance characteristics of these actuator structures.

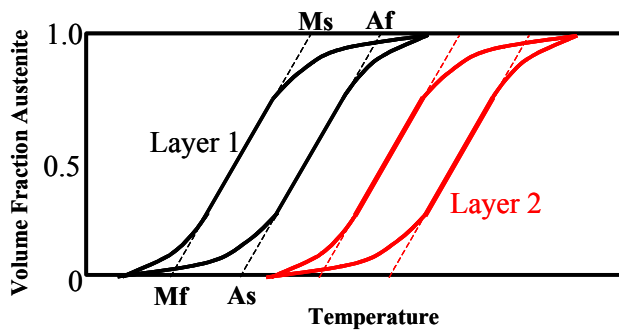
The TiNi alloys used for the SMA actuator structures developed here will be deposited using both RF-magnetron and Ion-beam sputter deposition techniques. We have the ability to co-deposit the alloy in both deposition processes. The standard RF-magnetron process should be suitable for deposition of the initial microstructures, studied in Phase-I of this program. However as we move to scale the systems down to sub-micron dimensions, we may require the added thickness uniformity and stoichiometry control that the Ion-beam deposition system provides. We have in place a system developed for the purpose of depositing alternating layers of nanometer thin-films for GMR applications that has the UHV cleanliness during deposition that these materials require. As seen in the left figure, the sputtered flux of the desired material is generated by an ion beam from an RF



ion source. The sputtered flux condenses on the substrate, which can be heated up to 700°C. The substrate rotation and target rotation systems are controlled by a LabView computer program, as are the ion gun and the substrate heater. A second RF ion beam gun is available for pre-cleaning, for bombarding the substrate during the film growth or for co-deposition from two targets as may be required for the TiNi system. We will apply this system should our magnetron-sputtered films in the sub-micron

range prove unsatisfactory.

Controlling SMA Transition Temperature: Sophisticated control of the transition temperature of SMA films is critical for the design of TAMS, both for actuation and for processing. For example, in the quest for sophisticated motion using a *uniform* thermal profile, we seek to control independent legs by varying the transition temperature for the SMA effect. As the temperature of the entire TAMS is raised, legs with the lower transition temperature will be actuated, leaving the highest temperature legs unchanged until later in the cycle when the temperature is high enough to leave all legs actuated. As discussed above, the actuation is generated by the strain induced from a martensite to austenite transition (upon heating) or the reverse upon cooling. The figure below is

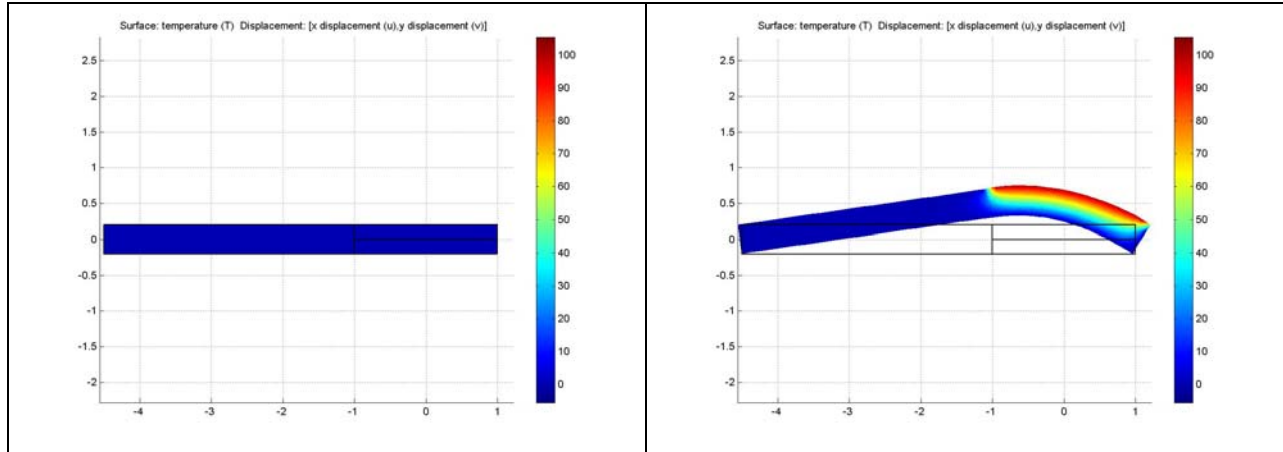


modified from Shih et al. [Shih 2001] and shows the basic transformation process. There is a transition temperature (A_s) at which the austenitic transformation starts and finishes (A_f) for the heating process. There are also corresponding transition temperatures for the martensitic (cooling) process, identified by M_s and M_f . Our proposed approach will be to develop alloy compositions with both low (one leg) and high (opposing) temperature transitions, as shown in the Layer 2 curve in the figure below. The material represented by these characteristics would even allow for independent modulation of one leg, independent of

the other by cycling the temperature through the higher or lower transition ranges respectively. In addition, these studies will be applied to graded alloy films for SMA thermal actuators, where the composition of the SMA film is varied through the thickness of the film. This film composition profile has been shown to be effective in both creating pre-bent structures and in thermal actuation [Gill2001]. Using our in-situ joule heating test structures with SEM imaging, we will measure the mechanical and thermomechanical properties of the TiNi thin films using mechanical beam techniques [Florando1999].

Modeling:

The modeling and simulation efforts will start with the analysis of conventional, bi-layer materials, which rely on the difference in thermal expansion coefficients for mechanical response to thermal actuation. A typical analysis consists of the solution of the time-dependent thermo-mechanically coupled problem, which is illustrated for the case of a simply supported structure below. The left part of the structure, consisting of a uniform material, represents the body, while the right part is a bi-metal structure with different thermal expansion coefficients, representing the legs. Heating of the upper leg surface results in a bending deformation of these legs, lifting up the entire body. The temperature distribution and the resulting motion can be seen in the figure below.



The second step will focus on the implementation of a shape memory alloy model into the structure. These inherently non-linear materials provide the highest work output per volume from all known actuating mechanisms [Hollerbach 1992], and this advantage becomes even more pronounced the smaller the scale. In [Seelecke 1999], we have recently extended the model originally developed by [Achenbach, 1985,1989] to simulate SMA-based actuation. The model is time-dependent and, in addition, it features full thermomechanical coupling through the inclusion of an energy balance. This makes it particularly well-suited for an application in the context of TAMS. For details on modeling and simulation of SMA-actuated smart structures, see the recent review article [Seelecke2001].

In [Seelecke1998 and Seelecke2000], we have developed a finite element version of the model, which has been successfully implemented in several adaptive structures, like deformable airplane sections [Campanile1999]. Figure 7 illustrates its capabilities by showing a sequence of beam shapes, caused by the contraction of two individually heated SMA wire actuators mounted on the beam. The main goal of the second step will be to incorporate our model for isolated SMA actuators into the description of composite TAMS.

At both levels, linear and non-linear, we will address modeling issues for an isolated structure at first. We will then concentrate on modeling the thermal management, which is greatly influenced by the heat exchange with the environment, including the substrate. An interesting issue here might be an observed anomaly of the thermal expansion coefficient in thin layers, see, e.g., [Paik2001]. The last phase will deal with the mechanical contact problem, which – alike the heat exchange - becomes increasingly important at smaller scales due to the growing influence of the surface properties. We will be looking at stiction and adhesion phenomena, as described, e.g., in [deBoer1999]. We also intend to investigate the influence of van-der-Waals interaction terms, playing another dominant role at the nano-scale. Molecular Dynamics simulations will be used to derive correctly scaled laws for force and thermal terms.

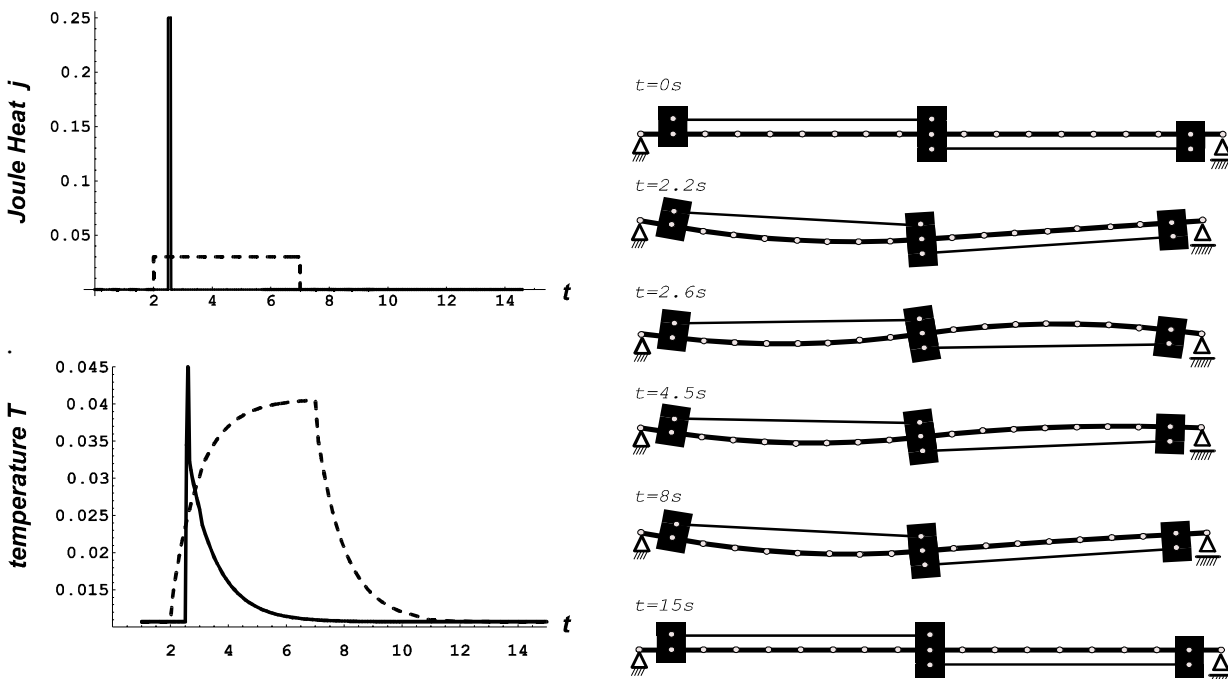


Figure 7 (Left-top) Heating functions for the two wires. Left wire: dashed line, right wire: solid line. (Left-bottom) temperatures, resulting from the heat pulses in Figure . Left wire: dashed line, right wire: solid line. (Right) Time sequence of bending in SMA wire structure due to heating and thermal profiles on left.

All of the above modeling efforts will greatly benefit from the experimental observations, which will be carried out in parallel. The measurements on transition temperatures of TiNi alloys, bending shapes within the SEM system (including time resolved shapes) and pre-stressed states will be incorporated into our continuing model development. This combination creates a unique environment to validate our modeling assumptions.

Conclusion: The control of mobile structures at the micro and nanoscale offers new opportunities for the control of the molecular scale world. With tools poised on the back of a microstructure, a mobile agent could assemble smaller structures, sample molecules, fix nanoconnections in circuitry. Scaling the mobile structure to the nanoscale carries all of these capabilities to even smaller realms, while opening up the possibility of considering the TAMS as an element of the circuitry or material itself. Challenges to be faced are the essence of Nanotechnology: how does the nanoworld differ from the microworld? How does the scaling of thermal transport, resonance frequencies, stiction, force generation and optical excitation dictate the geometry and materials for TAMS in the nanoworld? Our research will address these questions, and pursue new strategies from advanced materials to push this frontier.

Project Goals and Roles of PIs

3 Year Project Goals			
	TAMS	Adv. Materials	Modeling
Year 1	Define initial TAMS shapes and their actuation in test structures.	Establish polarization/antenna properties of NT. Demonstrate submicron thin film growth of SMA	Model thermomechanical dynamics of isolated TAMS.
Year2	Demonstrate TAMS actuation on surfaces as independent structures. Begin incorporation of SMA films in TAMS	Demonstrate thermal actuation of NT/metal structures. Demonstrate actuation of submicron SMA films	Incorporate thermal losses to substrate and van der Waals surface interactions
Year3	Begin incorporation of SMA films into nano-TAMS	Demonstrate SMA/NT structures as scaling route to nano-TAMS.	Incorporate stiction for full TAMS dynamic model.

Superfine brings expertise in nanoscale structures, forces and microscopy. He has developed photothermal actuation methods for scanning probe microscopy with a patent for its application to AFM imaging in liquid. He will direct the definition of TAMS geometries, and the actuation strategies and characterization. He will also coordinate the model development with thermomechanical measurements. Falvo has several years experience using scanning probe techniques to study the mechanical, electrical and friction properties of nanometer scale materials including the development of a combination SEM/AFM system. He will study the optical properties of the TAMS, design experiments for the measurement of actuation in electron, AFM and optical microscopes. Washburn has 15 years of experience in electron transport in nanoscale systems, nanometer-scale lithography and semiconductor processing. Washburn will oversee the processing and lithography of the TAMS. Brian Stoner has 10 years experience in the synthesis of advanced materials. He will concentrate on the growth of SMA thin films (TiNi alloys), and the correlation between their structure and actuation properties. He will work both using MCNC facilities and his laboratory at UNC. Stoner will take on one graduate student who will benefit from the experience of working in a non-academic laboratory setting (MCNC). Stefan Seelecke has expertise in the modeling of active materials including magnetic active and shape memory alloys. He will direct the effort in FEA modeling of TAMS including the thermomechanical behavior, thermal transport to ambient and to the substrate, van der Waals surface forces and actuation.

Management Strategy: We will hold biweekly team meetings between all P. I.'s alternating between UNC, NCSU and MCNC. One student will be located at NCSU under the direction of Seelecke. A second student will focus on processing and will under the direction of Stoner, and adjunct professor at UNC. Stoner has an office at UNC in the department of physics and astronomy and is on campus at least twice a week. Therefore, communication between this student, traveling between MCNC and UNC (a 15 minute drive), and the other P.I.'s and students at UNC will be transparent. The personnel under this project will participate in a weekly "device meeting" where we coordinate the activities in the laboratory across our device projects, and a weekly "nanoscience research group meeting" where all of the group's activities, including biophysics and microscopy development are brought together.

Integration of Research and Education

This project closely coordinates with the nanoManipulator project, an interdisciplinary group which pursues the development and application of advanced interfaces and techniques for scanning probe microscopy. It comprises about 25 people, including professors, postdoctoral fellows and graduate students from Computer Science, Physics, Chemistry, Health Sciences, Information and Library Science and Education. The students in this group work closely with colleagues with very different perspectives on their science and instrumentation.

Collaborations between UNC and MCNC are extensive with Brian Stoner being an adjunct professor at UNC. The students in the project will travel between MCNC (a 15 minute drive) on a weekly basis for processing and team meetings. Over 20 doctoral and 10 masters students have performed a significant portion of their dissertation research at MCNC and they currently have two full-time graduate students working on-site and, most important, have two *prior* students on our full-time research staff.

At NC State, the research will perfectly blend into the efforts to establish a new thrust area in Adaptive Systems. Seelecke has been hired to launch a program in Multifunctional Structures, and recently, the department

has proposed a new Ph.D. program in Intelligent and Adaptive Systems to NSF's IGERT program. Several new courses will be developed in this area like "Adaptive Structures I – Active Materials", which will be offered next semester by Seelecke. These courses will greatly benefit from such an interesting research topic and be more attractive to students

Our research group has also actively participated in minority recruitment. We have participated over the past 5 years in a campus program, Summer Pre-Graduate Research Experience, which brings excellent, junior-year minority students from across the U.S. to UNC to join research groups for the summer. They are then encouraged to apply to UNC for their graduate work. We have had 5 students from this program work within our microscopy research, and two have joined the group as graduate students, representing the first minority graduate students in our department in nearly 2 decades. One of these students, Phillip Williams, would be supported under this grant.

How can we get K-12 students interested in science? The advanced pen-controlled interface, the nanoManipulator, is of demonstrated scientific value. It is also great fun. We have taken the haptics interface and moderate graphics capability to a high school 15 miles away from the university. The AFM microscope and virus samples were located at UNC. The microscope and the user interface at the high school were connected using a T-1 network connection. The students were taken through a 3-hour program of instruction, model building, and hands-on operation of the AFM through the nanoManipulator interface. The proposed project will also participate in this program and the students will travel to area schools introducing them to nanoscale science and manipulation.

Results from Prior NSF Support

Richard Superfine, P. I.

Mechanical Properties of Nanotubes: Elastic Moduli, Buckling and a Nm-Scale Switch

NSF-ECS 9700677

\$419,854

7/1/97 - 6/30/01

Nanotube Dynamics: Atomic Lattices as Gears: We have studied the nanotube/substrate interaction through manipulation experiments. These studies have identified the full set of object dynamics, including stick/slip, sliding and rolling. The latter is the first observation of rolling in a nanometer scale system (see Figs. 5, 6). We have identified energy loss in rolling and compared it to the loss incurred in sliding. Most important, we have identified that the interlocking of the atomic lattices is responsible for the rolling. In other words, the atomic lattice is acting like a gear. **Compression/Strain -Conductivity Studies:** We have begun the study of the effects of strain and compression on nanotube electrical properties through *in-situ*, real time measurements of nanotube conductivity *while applying strain with the AFM tip*. Multiwall nanotubes show are relatively insensitive to strain at zero bias. We have broken nanotubes in device configurations and shown that the conductance recovers after manipulating the nanotube back into contact. We are currently making measurements on single walled nanotubes, measuring full I-V curves under strain.



1. M.R. Falvo, G. J. Clary, A. Helser, R. M. Taylor II, V. Chi, F. P. Brooks Jr., S. Washburn and R. Superfine, "Nanometre-scale rolling and sliding of carbon nanotubes," *Nature*, v397, n6716, pp236-238 (1999).
2. D. Srivastava, D.W. Brenner, J.D. Schall, K.D. Ausman, M.F. Yu and R.S. Ruoff, "Predictions of Enhanced Chemical Reactivity at Regions of Local Conformation Strain on Carbon Nanotubes", *J. Phys. Chem. B*, in press
3. J.D. Schall and D.W. Brenner, "Molecular Dynamics Simulations of Carbon Nanotube Rolling and Sliding on Graphite", *Molecular Simulation*, in press.
4. S. Paulson, M. R. Falvo, N. Snider, A. Helser, A. Seeger, R. M. Taylor II, R. Superfine, S. Washburn, "In-situ resistance measurements of strained carbon nanotubes" *Appl. Phys. Lett.*, **75** (19) 2936 (1999).
5. D.W. Brenner, O.A. Shenderova and D.A. Areshkin, 'Quantum-Based Analytic Interatomic Forces and Materials Simulation', in *Reviews in Computational Chemistry*, K.B. Lipkowitz and D.B. Boyd, Eds., (VCH Publishers, New York, 1998), in press.
6. C. Bower, R. Rosen, L. Jin, J. Han and O. Zhou, "Deformation of carbon nanotubes in nanotube-polymer composites", *Applied Physics Letters*, Vol. 74, No. 22, 3317 (1999).
7. M. R. Falvo, G. Clary, A. Helser, S. Paulson, R. M. Taylor II, V. Chi, F. P. Brooks Jr, S. Washburn, R. Superfine, "Nanomanipulation experiments exploring frictional and mechanical properties of carbon nanotubes", *Microscopy and Microanalysis*, **4**, 504-512. (1998)
8. D.W. Brenner, J.D. Schall, J.P. Mewkill and O.A. Shenderova 'Virtual Design and Analysis of Nanometer-Scale Sensor and Device Components', *Journal of the British Interp. Society*, Vol. 51, pp. 137-144 (1998).

9. C. Bower and S. Suzuki and K. Tanigaki and O. Zhou, "Synthesis and Structure of Pristine and Cesium Intercalated Single-Walled Carbon Nanotubes", *Applied Physics A* 67, 47-52, 1998,
10. S. Suzuki and C. Bower and O. Zhou, "In-situ TEM and EELS Observations of Alkali Metal Intercalation with SWNT Bundles", *Chem. Phys. Lett.*, 285, 230-234, 1998
11. C. Bower, A. Kleinhammes, Y. Wu and O. Zhou, "Intercalation and Partial Exfoliation of Single-Walled Carbon Nanotubes by Nitric Acid", *Chem. Phys. Lett.*, 288, 481-486, 1998
12. L. Jin, C. Bower and O. Zhou, "Alignment of carbon nanotubes in a polymer matrix by mechanical stretching", *Applied Physics Letter*, Vol. 73, No. 9, 1197 (1998).
14. O. Zhou, C. Bower, L. Jin, S. Suzuki and K. Tanigaki, "Carbon nanotubes: synthesis, processing and intercalation", in *Fullerenes: Recent Advances in the Physics and Chemistry of Fullerenes and Related Materials*, Vol. VI, 875-887 (Pennington: Electrochemical Society, 1998).
15. Falvo, M.R., G.J. Clary, R.M. Taylor II, V. Chi, F.P. Brooks Jr., S. Washburn and R. Superfine, "Bending and buckling of carbon nanotubes under large strain," *Nature*, Vol 389, No 6651, 1997, pp. 582 (cover story).

Michael Falvo, Co P. I.

Carbon Nanotube Nanoelectromechanical Devices: GHz signal processing, atomic scale position encoder

NSF-ECS SGER

\$59,000

8/31/00 – 9/1/01

Dynamics and electron transport at atomic interfaces: The carbon nanotube offers many opportunities for fundamental studies due to its apparent crystalline surface that is relatively immune to chemical degradation. We

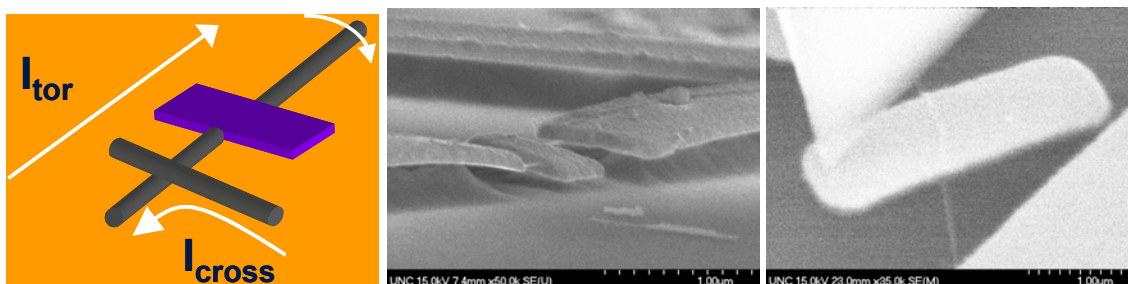


Figure 8. The paddle oscillator geometry can allow us to measure the current along a nanotube or across a nanotube junction while it is under torsional strain, providing insight into the coupling between chirality and transport with applications as a frequency source and force sensor. Fabricated nanotube paddle oscillator (center) using ebeam lithography and oxide etching/critical point drying for suspension. The AFM tip within our combination SEM/AFM system is manipulated to press on a suspended paddle for the measurement of torsional constants.

have placed nanotubes into contact with a variety of surfaces to study how nanoscale objects move under applied loads. This research is critical in understanding the limits for actuation and mechanical phenomena in atomic and molecular systems. In a series of studies, we manipulated nanotubes using an Atomic Force Microscope connected to our unique manipulation interface, the nanoManipulator, that allows the user to have pen-based control over the motion of the AFM tip. We found that the nanotube rolled only on graphite, and only when the atomic lattices were interlocked. The interlocking of atomic lattices has important implications for the electron transport across interfaces. We have used a metallized AFM tip placed on top of a carbon nanotube that itself was upon a graphite substrate. We measured the resistance as the current flowed from the tip, into the nanotube and finally into the substrate. By manipulating the nanotube, we could arrange it in arbitrary direction in the graphite surface. We can independently identify when the atomic lattices were interlocked by observing the friction between the nanotube and the surface. The resistance between the nanotube and the substrate decreased by a factor of 50 below its resistance when the lattices were out of registry. To our knowledge, this is one of the first demonstrations of momentum conservation in electron transport at an interface.

New nanoscale devices: We have begun the definition of oscillators based on carbon nanotubes that will allow fundamental measurements of torsional mechanical properties and potential nanoscale frequency references. We have applied ebeam lithography, wet etching of silicon oxide underlayers and critical point drying to create metal paddles suspended on carbon nanotubes. We have maneuvered our AFM tip within our SEM/AFM system to press on these freed paddles, and will use this methodology to measure torsional constants, and the correlation of transport with torsional strain and the interlocking of crossed nanotubes junctions. Finally, we have begun the design of combination nanotube/MEMS devices. In the simplest case, we have designed a MEMS structure to use as a stress/strain stage for nanotubes, in collaboration with Mike Sinclair of Microsoft Research. We have demonstrated

the ability to place a nanotube across a MEMS structure by pulling a nanotube from a loaded “cartridge” and placing the nanotube across the gap of a device. The nanotube is affixed at each side with carbon deposited by the electron beam which has been caused to dwell over the contact region.

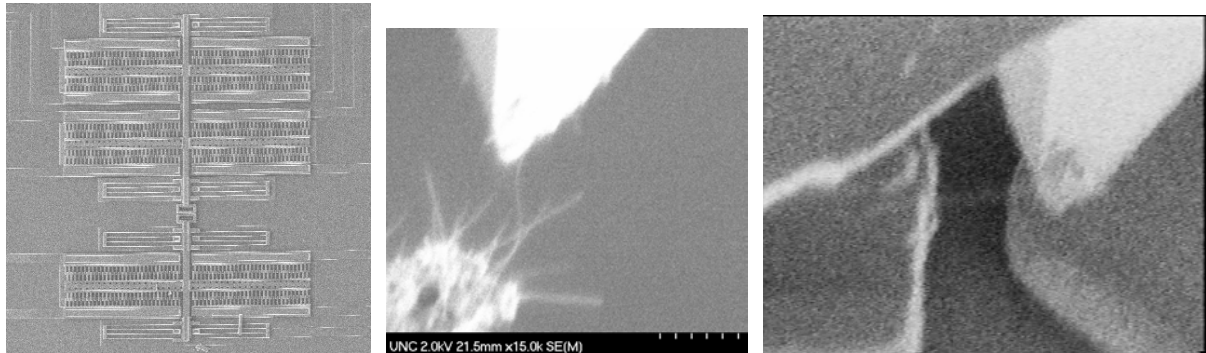


Figure 9. (Left) We have developed MEMS devices for nanoscale stress strain measurements using the MUMPS process at Cronos Inc. (JDS Uniphase). By plucking a nanotube from a “cartridge” of nanotubes (center), we can use an AFM tip within our SEM/AFM system to place the nanotube across a MEMS structure for subsequent tests (right).

Publications:

26. *Tunable resistance of a carbon nanotube-graphite interface*, S. Paulson , M. Falvo, M. Buongiorno Nardelli, R.M. Taylor II, A. Helser, R. Superfine, S. Washburn Science **290**: 1742-1744 (2000).
27. *Lattice Interactions in carbon nanotubes*, Falvo, M., R. Superfine, Tribology Lett 9, 73-76 (2000)
28. *Nanomanipulation for Physical Properties*, Falvo, M. and R. Superfine, J. Nanoparticle Research (invited review) 2, 237-248 (2000).
29. *Gearlike rolling motion mediated by commensurate contact: Carbon nanotubes on HOPG*, Falvo, M. R., J. Steele, R. M. Taylor II and R. Superfine, Phys. Rev. B **62**(16): R10,665-10667. (2000)

Sean Washburn, Co P. I.

Application of High-Performance Graphics Supercomputers and Communication to Provide Improved Interfaces to Scanning Probe Microscopes

NSF-ASC-9527192. \$2,300,000 Sept 1995-Aug 2000

We have developed several systems that place the user in control of the AFM tip using a force feedback pen and advanced real-time graphics for the visualization of the data. These systems include a standard ambient microscope, as well as a combination SEM/AFM system. **nanoWorkbench**: All components have been assembled and the system is in use by the scientists. Head tracking and haptic feedback allow users to see and feel the surface as if it is floating in front of them, magnified 1 million times. **Multi-modal Visualization**: We have developed two promising and complementary techniques for the visual display of multiple scalar fields on a surface. The first technique (which can only be implemented in real time on the PixelFlow graphics supercomputer) uses bump and dot patterns of different colors and sizes as its channels. The dots form clear regions on the surface, indicating where each data set has high values. This can be seen in the image to the left where the presence of each pattern indicates areas of high value from one data set from 9 SEM elemental analysis. Areas of overlap can be directly observed. We have also developed haptic visualization techniques.

Systems installed: Arizona St. Univ., NIST and Wright Patterson AFB, K. U. Leuven (Belgium).

Recent Publications (from 1998-1999) (see also above references)

16. Superfine, Richard, Michael R. Falvo, Scott Paulson, Sean Washburn, Russell M. Taylor II, G.J. Clary, Vernon Chi and Frederick P. Brooks, Jr., "Manipulation of Nanometer Objects: Friction, Mechanical Properties and Devices," Proceedings of the International Conference on Novel Materials, Puri, India (March 3-7, 1997)
17. Chen, Jun, Chris DiMattia, Mike Falvo, Pichet Thiansathaporn, Richard Superfine and Russell M. Taylor II, "Sticking to the Point: A Friction and Adhesion Model for Simulated Surfaces," Proceedings of the Sixth Annual Symposium on Haptic Interfaces for Virtual Environment and Teleoperator Systems, Dallas, Texas. November 17-18, 1997. pp. 167-171.
18. Taylor, Russell M., Jun Chen, Shoji Okimoto, Noel Llopis-Artime, Vernon L. Chi, Frederick P. Brooks, Jr., Mike Falvo, Scott Paulson, Pichet Thiansathaporn, David Glick, Sean Washburn and Richard Superfine, "Pearls

- Found on the way to the Ideal Interface for Scanned-probe Microscopes," Proceedings of IEEE Visualization '97, Phoenix, AZ, October 19-24, 1997. pp. 467-470.
19. M. R. Falvo, S. Washburn, R. Superfine, M. Finch, F. P. Brooks, Jr., V. Chi, and R. M. Taylor II, "Manipulation of Individual Viruses: Friction and Mechanical Properties," *Biophysical J.*, V. 72 No. 3, March 1997, pp. 1396.
 20. M. Falvo, R. Superfine, S. Washburn, M. Finch, R. M. Taylor, V. L. Chi, F. P. Brooks Jr., "The Nanomanipulator: A Teleoperator for Manipulating Materials at the Nanometer Scale ", Proceedings of the International Symposium on the Science and Technology of Atomically Engineered Materials (Richmond, VA , Oct 30 - Nov 4, 1995). World Scientific Publishing. 1996. pp. 579-586.
 20. Taylor II, Russell M. and Richard Superfine, "Advanced Interfaces to Scanned-Probe Microscopes," in Handbook of Nanostructured Materials and Nanotechnology, edited by H.S. Nalwa. Academic Press. Volume 2, Chapter 5. 1999. pp. 271-308.
 21. Grant, Brian, Aron Helser and Russell M. Taylor II, "Adding Force Display to a Stereoscopic Head-Tracked Projection Display," to appear in the proceedings of VRAIS '98, Atlanta, Georgia, 1998.
 22. "Quantitative Manipulation of DNA and Viruses with the nanoManipulator Scanning Force Microscope," Martin Guthold, W. Garrett Matthews, Atsuko Negishi, Russell M. Taylor II, Dorothy A. Erie, Frederick P. Brooks Jr, and Richard Superfine (1999) *Surf. Interf. Anal.* (In press)
 23. Gregory, Arthur, Ming C. Lin, Stefan Gottschalk and Russell Taylor, "A Framework for Fast and Accurate Collision Detection for Haptic Interaction," Proceedings of IEEE VR'99, Houston, Texas, March 13-17. pp. 38.
 24. R. M. Taylor II, "Haptic Visualization," in Human and Machine Haptics, M. A. Srinivasan, Ed., (MIT Press, 1999) *in press*.
 25. Taylor, Russell M., "Molecular Simulation and Microscope Control Applications of Force Feedback", course notes for *SIGGRAPH '98 Course #1*, "Physical Interaction: The Nuts and Bolts of Using Touch Interfaces." July 1998. 15 pages.